Phase transitions in self-assembled monolayers of alkanethiols containing the polar group

Y. V. Sukhinin*)

L. V. Kirensky Institute of Physics Russian Academy of Sciences, 660036 Krasnoyarsk, Russia
(Submitted 8 August 1997)
Zh. Éksp. Teor. Fiz. **114**, 208–221 (July 1998)

Equilibrium states of the system of self-assembled monolayers (SAMs) of *n*-alkanethiol molecules $HS(CH_2)_{n-1}(X)$ with polar group X chemiabsorbed on the Au(111) crystal surface are considered. The couplings between the atoms (C, H) of the *n*-alkanethiols are approximated by the Lennard–Jones potential. The couplings between the *n*-alkanethiols and the crystal surface are approximated by the 12-3 potential. The interactions of polar groups and the self-images with the metal substrate are taken into consideration. The phase-transition temperatures, the structural order and equilibrium tilt, and the twist and azimuthal angles of the macromolecules, which depend on the dipole moments, are found. © *1998 American Institute of Physics.* [S1063-7761(98)01507-8]

1. INTRODUCTION

The self-assembled monolayers (SAMs) are a comparatively new type of organic monolayers,[1–3] which are formed by spontaneous chemisorption of long-chain molecules from a solution to many different solid substrates (e.g., Au, Ag, Cu, Al, GaAs, and Si). The self-assembled monolayers are presently the focus of considerable attention for technological and fundamental reasons. They have potential applications in such areas as corrosion prevention, wear protection, sensing devices, and the formation of well-defined microstructures.[1,4,5] They also present an excellent opportunity for the study of two-dimensional, condensed, organic solids at the microscopic level. Chemisorption of the thiol headgroup to the surface results in long-range translational and orientational lattice structures. The stable monolayers have been studied extensively by transmission electron spectroscopy,[6–9] optical ellipsometry,[10–12] infrared spectroscopy,[13,14] electrochemistry,[15,16] and helium diffraction.[17,18] These monolayers form at a fixed surface density, which remains nearly constant with changing temperature. This fact simplifies the study of rotational and conformational states of SAMs.

The most thoroughly studied and robust SAM system is $CH_3(CH_2)_{n-1}SH$ adsorbed on the Au(111) crystal surface. Theoretical investigations of its properties have provided important insight into the nature of the long-range orderings of SAMs. To the extent possible, phenomenological methods,[19,20] molecular dynamic (MD) simulations,[21–26] and models of the SAMs such as the two-dimensional Ising model[27,28] have explained the ground state structure and thermal-equilibrium orientational states of the SAM. One of the objectives is to study SAMs with more complex molecular chains, i.e., self-assembled monolayers of alkanethols that contain a polar group. Molecular dynamic simulations of Langmuir–Blodgett monolayer with dipole group have already been considered.[29,30] However, these simulations, which are based on the so-called united atom model that treats CH_2 groups as single interaction sites, and allowance for the packing patterns of alkyl chains with one or two molecules per unit cell, give rise to an incorrect monolayer structure, the tilt angle, and tilt direction for zero dipole moment.

In this paper we are considering the effect of incorporating the polar group into self-assembled alkanethiol monolayers on the phase transitions and the molecular structure of the phases. We use an all-atom model for hydrocarbon chain interactions. In order to avoid gauche or kink defect in alkyl chains we placed the polar group at the end of the chains.

2. MOLECULAR MODEL

The model describes the *n*-alkanethiol rigid chains that terminate the polar group. The SH headgroups of the alkanethiols form a $(\sqrt{3}\times\sqrt{3})R30°$ triangular lattice to adjust with (coordinate) Au(111) substrate. An all-atom model includes hydrogen which is connected by rigid-bond couplings. This model is based mainly on the molecular model which was accepted by Hautman and Klein[22,23] and Mar and Klein,[24] except for the interactions between the chains. The chain has a zig-zag form and consists of hydrocarbon groups CH_2, which begin with sulfur and end with a polar group which a dipole moment **d** directs along the chain axis. We assume that arbitrary dipole moment belongs to the molecular group CH_3. Hydrocarbon groups CH_2 and CH_3 are represented by single interaction sites that include hydrogens. We assume that the chain may freely rotate about the chain axis as a whole with the twisting angle as the dihedral angle between the plane consisting of the normal to the gold surface, and the chain axis and plane defined by trans segments of the zig-zag molecular chain. We also assume that the chain may rotate relative to the crystal surface in such a way that the sulfur does not take part in this rotation. This rotation is determined by two angles: the tilting angle θ and the tilt direction φ (the precession angle of the long molecular axis about the surface normal to the gold crystal surface) (Fig. 1).

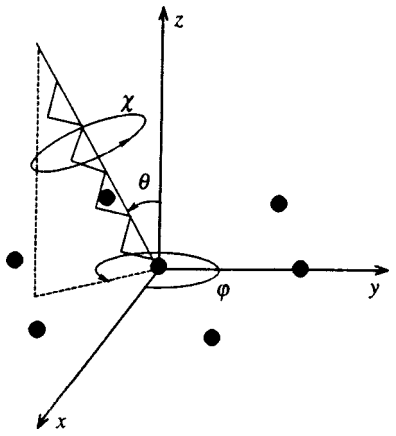

FIG. 1. θ is the tilt angle of the molecule, χ is the chain twist (rotation) angle, and φ characterizes the tilt direction along the surface plane.

Following Ref. 27, let us consider the Lennard–Jones interactions between the atoms H, C, and S

$$U(R)=4\epsilon\left[\left(\frac{\sigma}{R}\right)^{12}-\left(\frac{\sigma}{R}\right)^{6}\right]. \tag{1}$$

The Lennard–Jones (LJ) parameters ϵ and σ were chosen by fitting the potentials (1) to the van der Waals (vdW) potential $\exp(-r^{-6})$ in such a way that the potentials would have the same position, depth, and second derivatives at the point of minimum of the potentials. These parameters are listed in Tables I and II. We used the LJ potential since the vdW potential has a negative divergence for small distances, which means that all chains have a tendency to collapse on each other.

Following Hautman and Klein,[22] the interaction of the hydrocarbon groups CH_2 and CH_3 with the Au substrate was modeled by the 12-3 potential

$$V(z)=\frac{C_{12}}{(z-z_0)^{12}}-\frac{C_3}{(z-z_0)^3}, \tag{2}$$

where $C_{12}=2.8\times10^7$ K Å^2, $C_3=17100$ K Å^3, and $z_0=0.86$ Å.

The dipole–dipole coupling of the dipoles $\mathbf{d}_i$ and $\mathbf{d}_j$ is

$$W(\mathbf{R}_{ij})=\sum_{\alpha,\beta} W_{ij}^{\alpha,\beta} d_i^{\alpha} d_j^{\beta}, \tag{3}$$

where

$$W_{ij}^{\alpha,\beta}=\frac{\delta_{\alpha,\beta}}{R_{ij}^3}-\frac{3R_{ij}^{\alpha}R_{ij}^{\beta}}{R_{ij}^5}, \tag{4}$$

and $\mathbf{R}_{ij}$ is the vector between the dipole moments; the magnitude of a dipole moment is measured in units of $1D=4.8\times10^{-18}$ CGSE·cm.

The coordinates of the kth carbons in the local coordinate system with $\theta=0$, $\varphi=0$, and $\chi=0$ for the zig-zag chain in Fig. 2 are

$$\mathbf{R}_{Ck}=\begin{cases}(r,\ 0,\ l_0+(k-1)l/2), & k=1,3,5,\ldots,\\ (0,\ 0,\ l_0+(k-1)l/2), & k=2,4,6,\ldots,\end{cases} \tag{5}$$

where the distances in the chain are shown in Fig. 2, and χ is the twisting angle. The coordinates of the hydrogen are

$$\mathbf{R}_{Hks}=\begin{cases}(r+h\cos\alpha,\ hs\sin\alpha,\\ (-h\cos\alpha,\ hs\sin\alpha,\\ l_0+(k-1)/l/2), & k=1,3,5,\ldots,\\ l_0+(k-1)l/2), & k=2,4,6,\ldots.\end{cases} \tag{6}$$

The coordinates of the dipole are the same as those of C_n.

In order to find the coordinates defining the carbon and hydrogen atoms of the n-thiol chain in the coordinate system of the substrate, it is necessary to use the transformations of rotations determined by the Euler matrix

$$\mathbf{T}(\varphi,\theta,\chi)=\begin{pmatrix}\cos\varphi & -\sin\varphi & 0\\ \sin\varphi & \cos\varphi & 0\\ 0 & 0 & 1\end{pmatrix}\begin{pmatrix}\cos\theta & 0 & \sin\theta\\ 0 & 1 & 0\\ -\sin\theta & 0 & \cos\theta\end{pmatrix}\times\begin{pmatrix}\cos\chi & -\sin\chi & 0\\ \sin\chi & \cos\chi & 0\\ 0 & 0 & 1\end{pmatrix}.$$

This gives a transformation

$$\mathbf{R}(\varphi,\theta,\chi)=\mathbf{T}(\varphi,\theta,\chi)\mathbf{R}. \tag{7}$$

Experimental data[8,9] show that the chain is tilted to the next nearest neighbor (NNN) in the direction from the NNN direction ($\varphi\sim10°$). Below we consider the tilted phase ($\theta>0$) only. The number and equilibrium angular positions of the chains of the paraelectric phase depend on the symmetry of the system. We see that the one-body potential of the chain-S (1) and the chain-Au (2) is fourfold degenerate with respect to the angular positions of a chain $\mathbf{R}(\varphi,\theta,\chi)$, $\mathbf{R}(-\varphi,\theta,-\chi)$, $\mathbf{R}(\pi+\varphi,\theta,\chi)$, $\mathbf{R}(\pi-\varphi,\theta,-\chi)$. If the contribution of the potential of the chain from the straight chain of carbon atoms [in (5) $r=0$] is taken into account, then the chain-chain interactions (1) remove the mirror symmetry in the yz plane. Hence, the total one-body potential of a chain is twofold degenerate with respect to the angular positions

TABLE 1. Parameters of the van der Waals potential $A\exp(-Br)-C/r^6$.

A, 10^7 K			B, Å^{-1}			C, K Å^6			Refs.
A_{HH}	A_{HC}	A_{CC}	B_{HH}	B_{HC}	B_{CC}	C_{HH}	C_{HC}	C_{CC}	
0.33	1.4	6.0	4.08	4.08	3.08	2.5	6.3	16	31
1.50	1.5	1.5	5.00	4.13	3.42	2.2	7.0	21	32
1.10	1.1	1.1	4.64	3.94	3.42	2.7	7.2	17	33
0.92	1.1	1.3	4.64	3.94	3.42	2.2	6.9	19	34
0.46	6.8	2.1	4.54	4.56	3.58	2.1	6.4	20	35

TABLE II. The Lennard–Jones coupling parameters.

ϵ_{HH}, K	ϵ_{HC}, K	ϵ_{CC}, K	$\sigma_{0,HH}$, Å	$\sigma_{0,HC}$, Å	$\sigma_{0,CC}$, Å	Refs.
18	29	52	2.653	2.903	3.118	31
36	38	36	2.338	2.814	3.418	32
30	30	30	2.498	2.939	3.387	33
24	29	34	2.500	2.939	3.387	34
33	30	920	2.316	2.941	1.842	35

$\mathbf{R}(\varphi,\theta,\chi)$ and $\mathbf{R}(-\varphi,\theta,-\chi)$. This degeneracy was shown quantitatively in Ref. 27. The equilibrium state of the chains $\mathbf{R}(\varphi_0,\theta_0,\chi_0)$ and that of the mirror plane xz $\mathbf{R}(-\varphi_0,\theta_0,-\chi_0)$ is found from the minimum thermodynamic potential for $T>T_c$ and defined below.

In order to consider the phase transition with spontaneous breakdown of the symmetry we follow Vaks[36] and write the following expressions for the rotated coordinates of the atoms:

$$\begin{aligned}\mathbf{R}_s&=\mathbf{R}(s\varphi,\theta,s\chi)\\&=\frac{1}{2}\left[\mathbf{T}(\varphi,\theta,\chi)\mathbf{R}+\mathbf{T}(-\varphi,\theta,-\chi)\mathbf{R}\right]\\&\quad+s\,\frac{1}{2}\left[\mathbf{T}(\varphi,\theta,\chi)\mathbf{R}-\mathbf{T}(-\varphi,\theta,-\chi)\mathbf{R}\right]\\&=\mathbf{R}_\parallel+s\mathbf{R}_\perp,\quad s=\pm1.\end{aligned}\tag{8}$$

Obviously, since $\mathbf{R}_\parallel=(\mathbf{R}_{+1}+\mathbf{R}_{-1})/2$, $\mathbf{R}_\perp=(\mathbf{R}_{+1}-\mathbf{R}_{-1})/2$ and $|\mathbf{R}_{+1}|=|\mathbf{R}_{-1}|$,

$$\mathbf{R}_\parallel\mathbf{R}_\perp=0,$$

and $\mathbf{R}_\perp$ is directed along the y axis, as shown in Fig. 3. As the basis vectors of the two-dimensional triangular lattice of sulfur atoms we chose the vectors

$$\mathbf{a}_1=a(\sqrt{3}/2,1/2,0),\quad \mathbf{a}_2=(0,1,0),\tag{9}$$

where the lattice constant $a=4.97$ Å. Now let us specify the coordinates of the atoms of the jth chain on the surface:

$$\mathbf{R}_{jgk}=\mathbf{R}_j+\mathbf{R}_{\parallel,gk}+s_j\mathbf{R}_{\perp,gk},\tag{10}$$

where j runs over all sites of the triangular lattice, k runs over the atomic groups CH_2 and CH_3 along the chain, and g runs over the specific atomic groups ($g=$ C, H_1, and H_2). Accordingly, the dipole moment of the jth chain is

$$\mathbf{d}_j=\mathbf{d}_\parallel+s_j\mathbf{d}_\perp,\tag{11}$$

where $\mathbf{d}_\perp\parallel y$, and $\mathbf{d}_\parallel\mathbf{d}_\perp=0$.

Substituting expressions (8) and (10) into the potential interactions (1) and (2), we obtain the following expression for the LJ coupling chain-chain energy:

$$\begin{aligned}\frac{1}{2}\sum_{i,j}\sum_{g,g'}\sum_{k,k'}U_{gg'}(&\mathbf{R}_{ij}+\mathbf{R}_{0,gk}-\mathbf{R}_{0,g'k'}\\&+s_i\mathbf{R}_{1,gk}-s_j\mathbf{R}_{1,g'k'}),\end{aligned}\tag{12}$$

where $\mathbf{R}_{ij}=\mathbf{R}_i-\mathbf{R}_j$, and for the total chain-surface energy, which includes a coupling of the n-thiol atoms (C, H) with the sulfur atoms,

$$\begin{aligned}&\sum_i\sum_g\sum_k V(R^z_{0,k}+s_iR^z_{1,k})\\&\quad+\sum_{i,j}\sum_g\sum_{k,k'}U_{gS}(\mathbf{R}_{ij}+\mathbf{R}_{0,gk}+s_i\mathbf{R}_{1,gk}).\end{aligned}\tag{13}$$

In accordance with Eq. (1), we introduce the notation

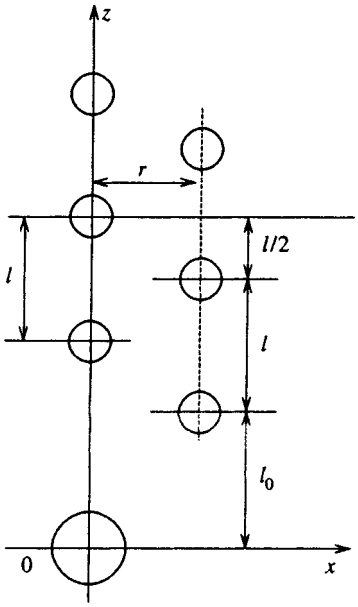

FIG. 2. Coordinates defining the model of the zig-zag n-thiol chain chemisorbed to a gold substrate; $l_0=1.58$ Å, $l=2.506$ Å, $r=0.878$ Å, $h=1.04$ Å, and $\alpha=55°$.

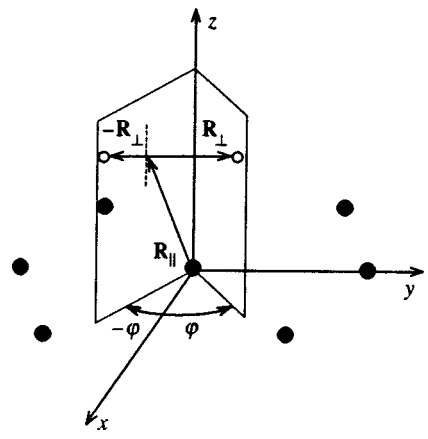

FIG. 3. Symmetrical positions of an atom of the n-thiol chains in the tilted phase.

$$U_{g,g'}=4\epsilon_{g,g'}\left[\left(\frac{\sigma_{g,g'}}{R}\right)^{12}-\left(\frac{\sigma_{g,g'}}{R}\right)^{6}\right], \tag{14}$$

and the notation $U_{g\mathrm{S}}$ means the interaction of the chain's atoms with the sulfur.

A single dipole spaced apart from a metal feels an interaction with its self-image, so a dipole-dipole part of the chain-chain energy consists of dipole-dipole, dipole-image and image-image interactions. Substituting expressions (9) and (10) into (3), we obtain the energy of the dipole-dipole coupling

$$\sum_{i,j}\left[W(\mathbf{R}_{ij}+(s_i-s_j)\mathbf{R}_{\perp,\mathrm{C}_n})+\frac{1}{2}\,W(\mathbf{R}_{ij}+\mathbf{Z}_{12}+(s_i-s_j)\mathbf{R}_{\perp,\mathrm{C}_n})\right], \tag{15}$$

where $\mathbf{Z}_{12}$ is the vector between the real dipole and its self-image.

In order to simplify expressions (12), (13), and (15) we introduce the projection operators $s^{\pm}=(1\pm s)/2$. Then for any function f of the two operators s_1 and s_2 there is an identity[36]

$$\begin{aligned}f(xs_1+ys_2)&=(s_1^+ +s_1^-)(s_2^+ +s_2^-)f(xs_1+ys_2)\\&=s_1^+s_2^+f(x+y)+s_1^+s_2^-f(x-y)\\&\quad+s_1^-s_2^+f(-x+y)+s_1^-s_2^-f(-x-y).\end{aligned} \tag{16}$$

Using this identity, we can write the following expression for the total energy of the SAM:

$$E=E_0-\frac{1}{2}\sum_{ij}J_{ij}(\theta,\varphi,\chi)s_is_j. \tag{17}$$

In accordance with Eq. (16), we obtain the expressions

$$E_0=\frac{1}{4}\sum_{ij}\sum_{s,s'}(U^{ij}_{s,s'}+W^{ij}_{s,s'})+\frac{1}{2}\sum_i\sum_s V^i_s, \tag{18}$$

$$J_{ij}=\frac{1}{4}\sum_{s,s'}ss'U^{ij}_{s,s'}+\frac{1}{4}\sum_{s,s'}ss'W^{ij}_{s,s'}, \tag{19}$$

where

$$\begin{aligned}U^{ij}_{s,s'}&=\frac{1}{2}\sum_{gg'}\sum_{kk'}U_{gg'}(\mathbf{R}_{ij}+\mathbf{R}_{\parallel,gk}\\&\quad-\mathbf{R}_{\parallel,g'k'}+s\mathbf{R}_{\perp,gk}-s'\mathbf{R}_{\perp,g'k'}),\\W^{ij}_{s,s'}&=W(\mathbf{R}_{ij}+(s-s')\mathbf{R}_{\perp,\mathrm{C}_n})\\&\quad+\frac{1}{2}\,W(\mathbf{R}_{ij}+\mathbf{Z}_{12}+(s-s')\mathbf{R}_{\perp,\mathrm{C}_n}),\\V^i_s&=\sum_g\sum_k V(R^z_{\parallel,k}+sR^z_{\perp,k})\\&\quad+\sum_j\sum_g\sum_k U_{g\mathrm{S}}(\mathbf{R}_{ij}+\mathbf{R}_{\parallel,gk}+s\mathbf{R}_{\perp,gk}).\end{aligned} \tag{20}$$

The linear term $\Sigma_iB_is_i$ is absent in Eq. (17) due to the symmetry.

3. MEAN-FIELD APPROXIMATION

According to (17), the thermodynamic potential of the SAM is

$$F=E_0(\theta,\varphi,\chi)-T\ \ln\mathrm{Tr}_{\{s_i\}}\times\exp\left[\frac{1}{2}\sum_{ij}J_{ij}(\theta,\varphi,\chi)\,\frac{s_is_j}{T}\right]. \tag{21}$$

A mean-field approximation of Eq. (21) is given by the expression[36]

$$F=E_0(\theta,\varphi,\chi)+\frac{1}{2}\sum_{ij}J_{ij}(\theta,\varphi,\chi)\langle s_i\rangle\langle s_j\rangle-T\sum_i\ \ln\left[2\cosh\left(\sum_j J_{ij}(\theta,\varphi,\chi)\,\frac{\langle s_j\rangle}{T}\right)\right]. \tag{22}$$

We see from Eq. (22) that in the paraelectric phase ($\langle s_i\rangle=0$) the minimum $E_0(\varphi,\theta,\chi)$ with respect to the angles gives equilibrium $\varphi_0,\theta_0,\chi_0$ SAM's chains. The order parameter $\langle s_i\rangle\neq0$ is defined as a solution of the equations of state[37]

$$\langle s_i\rangle=\tanh\left[\sum_j J_{ij}(\theta,\varphi,\chi)\,\frac{\langle s_j\rangle}{T}\right]. \tag{23}$$

A substitution of solutions of this equation into (22) and self-consistent minimization of the thermodynamic potential over three angles give the complete equilibrium state of the SAM. Next, according to Eq. (23), the structure ordered phase is determined by the wave vector $\mathbf{q}_0$, for which

$$J_{\mathbf{q}}=\sum_j J_{ij}\,\exp(i\mathbf{q}\mathbf{R}_{ij}) \tag{24}$$

takes on the maximum value, and $T_c=J_{\mathbf{q}_0}$.[37]

The first item transform in (19) under nearest-neighbor chain-chain coupling is given by the expression[27]

$$U(\mathbf{q})=2J_1\cos(2\pi\xi_1)+2J_1\cos[2\pi(\xi_1-\xi_2)]+2J_2\cos(2\pi\xi_2), \tag{25}$$

where the wave vector $\mathbf{q}=\xi_1\mathbf{b}_1+\xi_2\mathbf{b}_2$ is written about the basis reciprocal to (9)

$$\mathbf{b}_1=4\pi a^{-1}(1/\sqrt{3},0,0),\quad \mathbf{b}_2=2\pi a^{-1}(-1/\sqrt{3},1,0), \tag{26}$$

J_1 is the coupling constant along the vectors $\pm\mathbf{a}_1$, $\pm(\mathbf{a}_2-\mathbf{a}_1)$, and J_2 is the coupling constant along the vectors $\pm\mathbf{a}_2$.

One points to fact that at $\mathbf{d}=0$ expression (24) reduces to (25), maximums which give the following structure ordered phase and the transition temperature:[27]

1) $\xi_1=0,\quad \xi_2=0,\quad T_c=4J_1+2J_2$ (ferro);

2) $\xi_1=0.5\quad \xi_2=0,\quad T_c=-4J_1+2J_2$ (2×1);

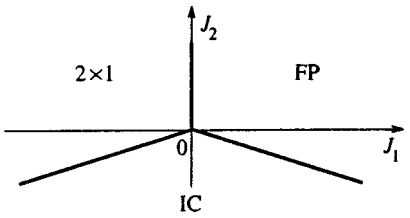

FIG. 4. Phase diagram of the Ising model on the triangular lattice.

$$3) \quad \xi_1 = 0.5\xi_2, \quad T_c = -\frac{J_1^2}{J_2} - 2J_2, \quad \left|\frac{J_1}{2J_2}\right| \leqslant 1 \quad \text{(IC)}. \tag{27}$$

The phase diagram, which corresponds to Eq. (27), is shown in Fig. 4.

The dipole-dipole interaction transform of (19) is computed by Ewald's method[38] by fitting to the $2D$ lattice. Formally, the Fourier transform (4) can be found as follows:

$$W^{\alpha,\beta}_{\mathbf{q},\mathbf{x}} = -\frac{\partial^2}{\partial x_\alpha \partial x_\beta} \sum_{\mathbf{l}} \frac{e^{i\mathbf{q}\mathbf{l}}}{|\mathbf{l}-\mathbf{x}|}, \tag{28}$$

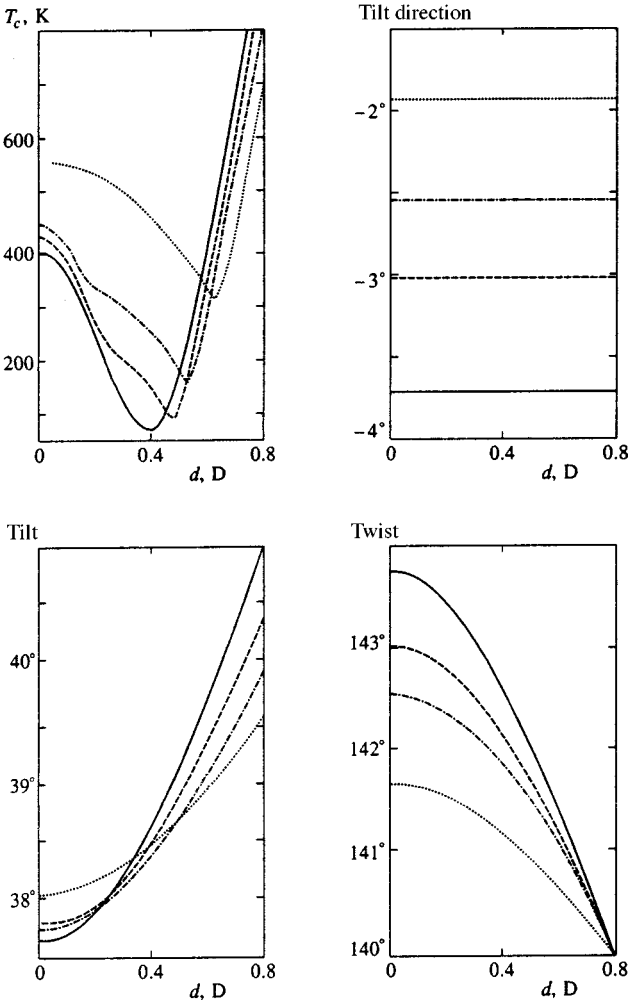

FIG. 5. Curves of the temperature transition T_c and the equilibrium angles of the n-thiols, plotted as functions of the dipole moment, are described by the solid ($n=8$), dashed ($n=10$), dot-dashed ($n=12$), and dotted ($n=17$) lines for the coupling parameters from Ref. 32.

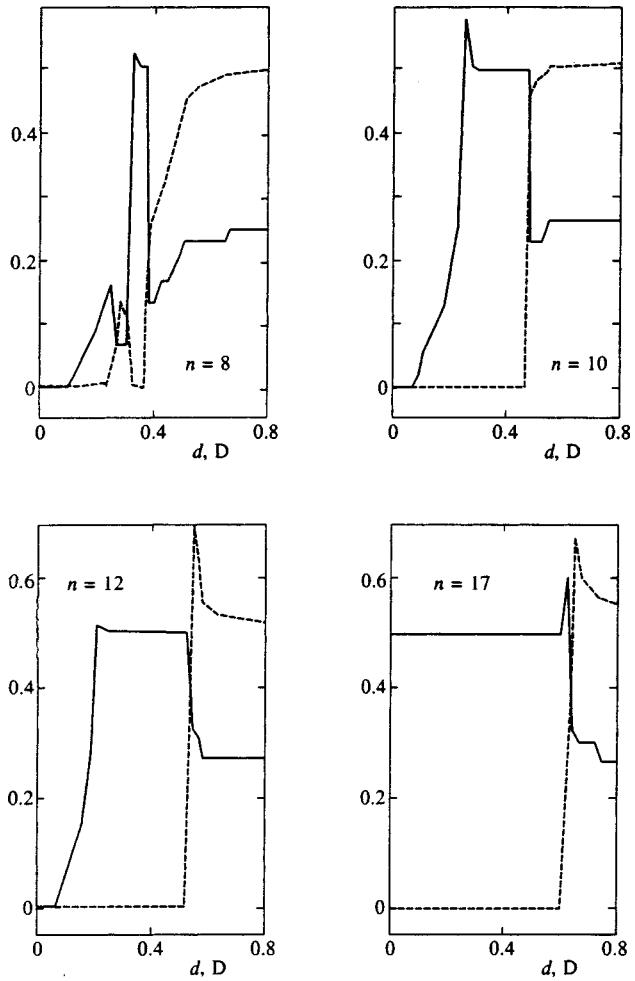

FIG. 6. The components of the wave vector of the ordered structure ξ_1 (solid) and ξ_2 (dashed) for the coupling parameters from Ref. 32.

where $\mathbf{l}=l_1\mathbf{a}_1+l_2\mathbf{a}_2, l_1, l_2$ is an integer, and $\mathbf{a}_1$ and $\mathbf{a}_2$ are defined by expressions (9). According to Ewald, the series of (28) for a plane lattice is presented by the sum of two series:

$$\sum_{\mathbf{l}} \frac{e^{i\mathbf{q}\mathbf{l}}}{|\mathbf{l}-\mathbf{x}|} = \sum_{\mathbf{l}} \frac{\operatorname{erfc}(R|\mathbf{l}-\mathbf{x}|)}{|\mathbf{l}-\mathbf{x}|} + \frac{\pi}{S_0} \sum_{\mathbf{g}} \frac{e^{i\mathbf{x}(\mathbf{q}+\mathbf{g})}}{|\mathbf{g}+\mathbf{q}|} \times \left[e^{z|\mathbf{q}+\mathbf{g}|} \operatorname{erfc}\left(\frac{|\mathbf{q}+\mathbf{g}|}{2\mathbf{R}} + zR \right) + e^{-z|\mathbf{q}+\mathbf{g}|} \operatorname{erfc}\left(\frac{\mathbf{q}+\mathbf{g}|}{2\mathbf{R}} - zR \right) \right], \tag{29}$$

where

$$\operatorname{erfc}(x) = \frac{2}{\sqrt{\pi}} \int_x^\infty e^{-y^2} dy.$$

Here $\mathbf{g}=g_1\mathbf{b}_1+g_2\mathbf{b}_2, g_1, g_2$ is an integer, $\mathbf{b}_1$ and $\mathbf{b}_2$ are defined by expressions (26), S_0 is the unit cell area, z is the component along the z axis of the vector $\mathbf{x}$, and R is the adjustable parameter of the velocity convergence of the series. Note that Eq. (29) was obtained in Ref. 29 for $\mathbf{q}=0$.

The results of self-consistent numerical minimization procedure of (22) are given in Figs. 5–8 and Table III. The first feature of the temperature transition is high sensitivity to

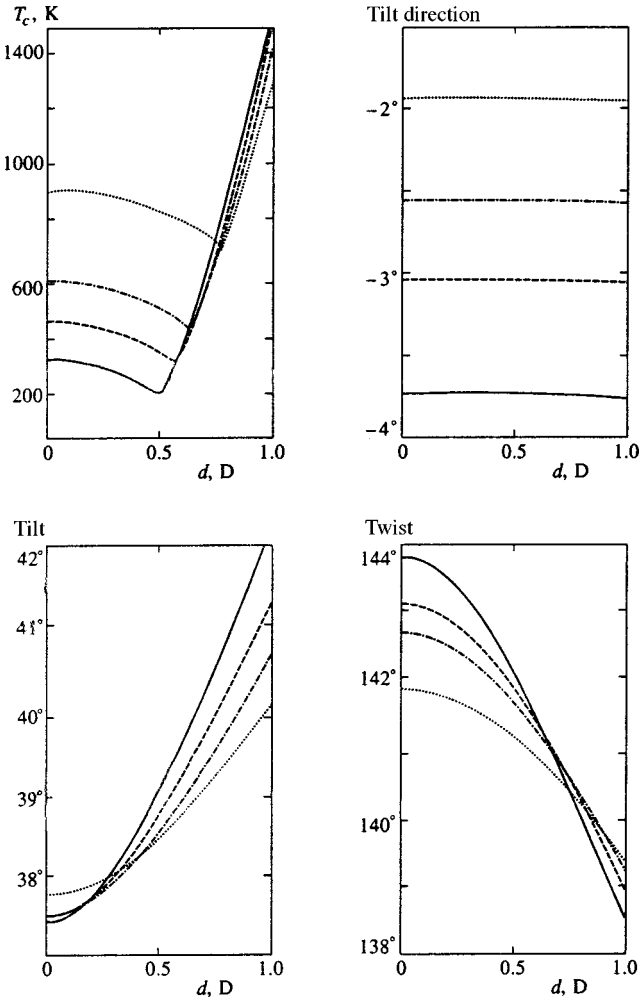

FIG. 7. The same as in Fig. 5 for Ref. 35.

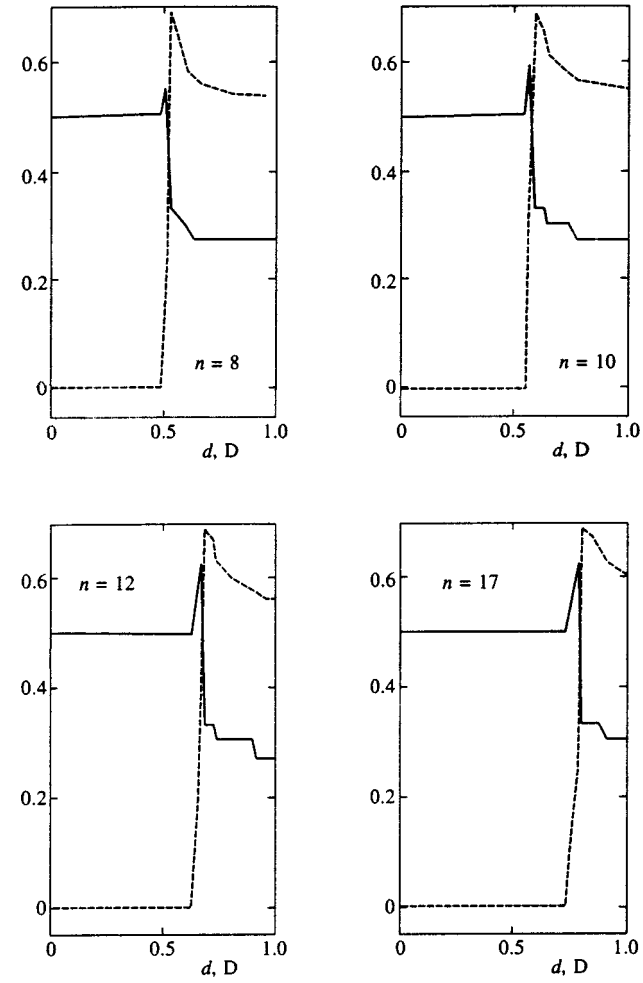

FIG. 8. The same as in Fig. 6 for Ref. 35.

the choice of the coupling constants listed in Table II. For the choice of the coupling constants defined in Refs. 32 and 35 there is ordered phase sequence from the ferroelectric or 2×1 to the IC (Figs. 6 and 8). However, for the choice of coupling constants defined in Refs. 31, 33, and 34 there is IC phase (Table III), where the transition temperature T_c increases with increasing dipole moment.

4. DISCUSSION AND CONCLUSIONS

An advantage of using the Ising variable is that a rich variety of the couplings between atoms of the *n*-thiols and the couplings with the crystal surface is reduced to a few competing exchange parameters. For $d=0$ they allow one to establish a simple phase diagram of the system shown in Fig. 4. The SAMs are described by the Ising model on the triangular lattice with exact solution.[39] Ferroelectric, 2×1, and incommensurate phases are the only possible ordered states of the system of the *n*-thiols which are self-assembled on the crystal surface Au(111). For $d\neq0$ competition a LJ interaction and a dipole-dipole coupling can give rise to various combinations of the structures.

The most interesting behavior of the critical temperature and a sequence of ordered structures upon change in the dipole moment has been found for the LJ's parameters from Refs. 32 and 35. The transition temperature dependence is that T_c with $d\neq0$ can be reduced when $d=0$. In particular, the lowest temperature of the phase transition is realized for the parameters taken from Refs. 32 and 34. T_c is very sensitive to the coupling parameters which change many times. Moreover, it is necessary to take into consideration that all coupling parameters listed in Table I are given for the case of three-dimensional crystals in which the distances between the atomic groups CH_2 may differ in comparison with the case of the SAM. Therefore, the coupling constants listed in Tables I and II should be considered carefully. As far as the structure of the ordered phase for any set coupling parameters is concerned, with increasing dipole moment the incommensurate phase is described by the modulation vector either near $\xi=(0.25,0.5)$ or near $\xi=(0.3,0.6)$.

The phase transition leads to a freezing of the jumps of the chains between twofold degenerate states with equilibrium azimutal and twist angles φ_0, and χ_0 is given in Figs. 5 and 7 and Table III for various references. The values of these angles agree with the experimental observations and theoretical considerations except for the azimutal angle which was determined experimentally to be $\varphi\sim10°$ for $d=0$ and $10<n<20$ (Ref. 9).

The final feature of the phase transition to the twisted

TABLE III. The critical temperatures, the wave vector, and the equilibrium angles.

n	T_c, K	ξ_1	ξ_2	θ_0	χ_0	φ_0	Refs.
$d = 0.5$ D							
8	1249.6	0.259	0.517	−3.88	35.55	143.75	31
12	1701.6	0.259	0.525	−2.68	35.11	142.95	"
16	2156.9	0.259	0.529	−2.05	34.90	142.50	"
8	688.5	0.259	0.520	−3.82	36.21	143.75	33
12	855.6	0.273	0.538	−2.64	35.80	143.00	"
16	1028.7	0.273	0.549	−2.02	35.61	142.58	"
8	619.7	0.259	0.525	−3.81	36.68	143.37	34
12	745.3	0.273	0.546	−2.63	36.23	142.69	"
16	878.0	0.273	0.561	−2.01	36.01	142.30	"
$d = 1.0$ D							
8	2857.1	0.253	0.510	−3.79	38.34	141.53	31
12	3224.2	0.259	0.519	−2.63	37.04	141.61	"
16	3642.2	0.259	0.524	−2.02	36.39	141.55	"
8	2227.0	0.253	0.512	−3.77	39.05	141.19	33
12	2311.7	0.267	0.524	−2.60	37.72	141.44	"
16	2442.9	0.267	0.532	−1.99	37.08	141.46	"
8	2154.5	0.267	0.516	−3.77	39.71	140.52	34
12	2200.6	0.267	0.528	−2.60	38.29	140.91	"
16	2290.4	0.267	0.537	−1.99	37.59	141.01	"

ordered phase is that it is a first-order transition. The reason is analogous to the effect of elastic media on the order of the phase transition,[36,40] where the spontaneous ordering gives rise to a distortion of the crystal, which in turn leads to a slight increase in the exchange integrals. Hence, the Curie temperature from the paraelectric phase turns out to be lower than the Curie temperature from the ordered phase. Similarly, in the system of the *n*-thiol's chains a spontaneous twist ordering of the chains give rise to a change in the tilt. This in turn leads to a change of the exchange integrals defined by Eq. (19).

I wish to thank A. F. Sadreev for valuable discussions and for stimulating interest. I also thank E. N. Bulgakov for his assistance in setting up the calculations. This work was supported by the Krasnoyarsk Regional Science Foundation Grant 6F0031.

*)E-mail: zeos@zeos.krascience.rssi.ru

[1] J. D. Swalen, D. L. Allara, J. D. Andrade *et al.*, Langmuir **3**, 932 (1987).
[2] L. H. Dubois and R. G. Nuzzo, Annu. Rev. Phys. Chem. **43**, 437 (1992).
[3] R. G. Nuzzo, F. A. Fusco, and D. L. Allara, J. Am. Chem. Soc. **109**, 2358 (1987).
[4] P. E. Laibinis and G. M. Whitesides, J. Am. Chem. Soc. **114**, 9022 (1992).
[5] A. Kumar, H. A. Biebuyck, and G. M. Whitesides, Langmuir **10**, 1498 (1994).
[6] L. S. Strong and G. M. Whitesides, Langmuir **4**, 546 (1988).
[7] C. E. D. Chidsey and D. N. Loiacono, Langmuir **6**, 682 (1990).
[8] P. Fenter, P. Eisenberger, and K. S. Liang, Phys. Rev. Lett. **70**, 2447 (1993).
[9] P. Fenter, P. Eisenberger, K. S. Liang, and A. Eberhard, J. Chem. Phys. **106**, 1600 (1997).
[10] C. D. Bain, E. B. Troughton, Y.-T. Tao *et al.*, J. Am. Chem. Soc. **111**, 321 (1989).
[11] G. M. Whitesides and P. E. Laibinis, Langmuir **6**, 87 (1990).
[12] S. D. Evans, E. Urankar, A. Ulman, and N. Ferris, J. Am. Chem. Soc. **113**, 4121 (1991).
[13] R. G. Nuzzo, L. H. Dubois, and D. L. Allara, J. Am. Chem. Soc. **112**, 558 (1990).
[14] R. G. Nuzzo, E. M. Korenic, and L. H. Dubois, J. Chem. Phys. **93**, 767 (1990).
[15] T. T. T. Li and M. J. Weaver, J. Am. Chem. Soc. **106**, 6107 (1984).
[16] M. D. Porter, T. B. Bright, D. L. Allara *et al.*, J. Am. Chem. Soc. **109**, 3559 (1987).
[17] N. Camillone III, C. E. D. Chidsey, G. Liu *et al.*, J. Chem. Phys. **94**, 8493 (1991).
[18] N. Camillone III, C. E. D. Chidsey, G. Liu *et al.*, J. Chem. Phys. **98**, 3503 (1993).
[19] R. Nagarajan and E. Ruckenstein, Langmuir **7**, 2934 (1991).
[20] V. M. Kaganer, M. A. Osipov, and I. R. Peterson, J. Chem. Phys. **98**, 3512 (1993).
[21] C. M. Knobler and R. C. Desai, Annu. Rev. Phys. Chem. **43**, 207 (1992).
[22] J. Hautman and M. L. Klein, J. Chem. Phys. **91**, 4994 (1989).
[23] J. Hautman and M. L. Klein, J. Chem. Phys. **93**, 7483 (1990).
[24] W. Mar and M. L. Klein, Langmuir **10**, 188 (1994).
[25] S. Shin, N. Collazo, and S. A. Rice, J. Chem. Phys. **98**, 3469 (1993).
[26] M. A. Moller, D. J. Tildesley, K. S. Kim *et al.*, J. Chem. Phys. **94**, 8390 (1991).
[27] A. F. Sadreev and Y. V. Sukhinin, Phys. Rev. B **54**, 17966 (1996).
[28] A. F. Sadreev and Y. V. Sukhinin, J. Chem. Phys. **107**, 2643 (1997).
[29] V. V. Kislov, Y. A. Kriksin, and I. V. Taranov, Radiotekh. Elektron. **38**, 539 (1993).
[30] V. V. Kislov, Y. A. Kriksin, and I. V. Taranov, Radiotekh. Elektron. **41**, 241 (1996).
[31] L. S. Bartell, J. Chem. Phys. **32**, 827 (1960).
[32] A. I. Kitaigorodsky, Tetrahedron **14**, 230 (1961).
[33] A. I. Kitaigorodsky, Molecular Crystals and Molecules, Academic Press, New York and London (1973), Chap. 2.
[34] A. I. Kitaigorodsky, Adv. Struct. Res. 3, 204 (1970).

[35] T. Wasiutyński and T. Luty, Acta Phys. Pol. A **45**, 551 (1974).
[36] V. G. Vaks, *Introduction to Microscopic Theory of Ferroelectrics*, Nauka, Moscow (1973) (in Russian).
[37] R. Blinc and B. Žekš, *Soft Modes in Ferroelectrics and Antiferroelectrics*, North-Holland Publ., Amsterdam (1974).
[38] J. M. Ziman, *Principles of the Theory of Solids, 2nd ed.*, Cambridge (1972).
[39] R. J. Baxter, *Exactly Solved Models in Statistical Mechanics*, Academic Press, New York (1982), Chap. 11.
[40] O. K. Rice, J. Chem. Phys. **22**, 1535 (1954).

Published in English in the original Russian journal. Reproduced here with stylistic changes by the Translation Editor.